

# Combination of Cetuximab and Oncolytic Virus Canerpaturev Synergistically Inhibits Human Colorectal Cancer Growth

Zhiwen Wu,<sup>1,2</sup> Toru Ichinose,<sup>1,2</sup> Yoshinori Naoe,<sup>2</sup> Shigeru Matsumura,<sup>2</sup> Itzel Bustos Villalobos,<sup>2</sup> Ibrahim Ragab Eissa,<sup>1,2</sup> Suguru Yamada,<sup>1</sup> Noriyuki Miyajima,<sup>1</sup> Daishi Morimoto,<sup>1</sup> Nobuaki Mukoyama,<sup>3</sup> Yoko Nishikawa,<sup>1</sup> Yusuke Koide,<sup>3</sup> Yasuhiro Kodera,<sup>1</sup> Maki Tanaka,<sup>4</sup> and Hideki Kasuya<sup>1,2</sup>

<sup>1</sup>Department of Surgery II, Nagoya University Graduate School of Medicine, 65 Tsurumai-cho, Showa-ku, Nagoya 466-8550, Aichi, Japan; <sup>2</sup>Cancer Immune Therapy Research Center, Nagoya University Graduate School of Medicine, 65 Tsurumai-cho, Showa-ku, Nagoya 466-8550, Aichi, Japan; <sup>3</sup>Otorhinolaryngology, Nagoya University Graduate School of Medicine, 65 Tsurumai-cho, Showa-ku, Nagoya 466-8550, Aichi, Japan; <sup>4</sup>Takara Bio Inc., 7-4-38, Nojihigashi, Kusatsu 525-0058, Shiga, Japan

**The naturally occurring oncolytic herpes simplex virus canerpaturev (C-REV), formerly HF10, proved its therapeutic efficacy and safety in multiple clinical trials against melanoma, pancreatic, breast, and head and neck cancers. Meanwhile, patients with colorectal cancer, which has increased in prevalence in recent decades, continue to have poor prognosis and morbidity. Combination therapy has better response rates than monotherapy. Hence, we investigated the antitumor efficacy of cetuximab, a widely used anti-epidermal growth factor receptor (EGFR) monoclonal antibody, and C-REV, either alone or in combination, *in vitro* and in an *in vivo* human colorectal xenograft model. In human colorectal cancer cell lines with different levels of EGFR expression (HT-29, WiDr, and CW2), C-REV exhibited cytotoxic effects in a time- and dose-dependent manner, irrespective of EGFR expression. Moreover, cetuximab had no effect on viral replication *in vitro*. Combining cetuximab and C-REV induced a synergistic anti-tumor effect in HT-29 tumor xenograft models by promoting the distribution of C-REV throughout the tumor and suppressing angiogenesis. Application of cetuximab prior to C-REV yielded better tumor regression than administration of the drug after the virus. Thus, cetuximab represents an ideal virus-associated agent for antitumor therapy, and combination therapy represents a promising antitumor strategy for human colorectal cancer.**

## INTRODUCTION

Colorectal cancer (CRC) is the third most common cancer worldwide<sup>1</sup> and one of the leading causes of cancer death in Japan.<sup>2</sup> Furthermore, the morbidity and incidence of this cancer are expected to be increased in the coming decades.<sup>3</sup> Although a variety of CRC treatments have been applied in the clinic, the efficacy of traditional treatment strategies (surgery or/and radiation therapy) is limited after long-term observation.<sup>4</sup> Accordingly, there is a desperate need for multimodal therapy to improve outcomes in patients with CRC.

Based on accumulating preclinical and clinical data, oncolytic viruses have been proposed as a promising and highly effective therapy for cancer treatment.<sup>5,6</sup> Among various oncolytic viruses, the oncolytic herpes simplex virus (oHSV) has several advantageous features, including highly efficient infection and broad host range. Talimogene laherparepvec (T-vec) is the first oncolytic virus approved by the FDA for the treatment of malignant melanoma.<sup>7</sup> Canerpaturev (C-REV) is a spontaneous mutant clone derived from HF, a highly attenuated mutant strain of HSV-1, which showed promise in our previous studies.<sup>8–15</sup> We applied C-REV to treatment of various kinds of solid tumors *in vitro* and *in vivo*, and we demonstrated safety and efficacy in preclinical and clinical studies.<sup>8–15</sup> In addition to our study with C-REV, other studies with oHSV exhibited enhanced angiogenesis, which might affect the inhibition of tumor growth.<sup>16–18</sup> Antiangiogenic effect should be considered as a critical factor in combination therapy with C-REV.

Epidermal growth factor receptor (EGFR) signaling is involved in apoptosis, angiogenesis, cell proliferation, migration, and invasion.<sup>19</sup> We previously applied a combination therapy of C-REV and erlotinib, an EGFR tyrosine kinase inhibitor, against human pancreatic cancer; the results revealed that erlotinib enhanced C-REV distribution within the tumor by inhibiting virus-induced angiogenesis.<sup>20</sup> Salomon et al.<sup>21</sup> reported EGFR overexpression (72%–82% above normal tissue) in CRC. Cetuximab, a monoclonal antibody that binds to the extracellular domain of EGFR, has been applied widely to suppress tumor growth. Inhibition of EGFR activation leads to downregulation of the RAS/RAF/MEK/ERK and PI3K/AKT pathways, which decrease vascular endothelial growth factor (VEGF) promoter activity. Inhibition of EGFR activity by cetuximab induces an

Received 9 October 2018; accepted 24 April 2019;  
<https://doi.org/10.1016/j.omto.2019.04.004>.

**Correspondence:** Hideki Kasuya, MD, PhD, FACS, Department of Surgery II, Nagoya University Graduate School of Medicine, 65 Tsurumai-cho, Showa-ku, Nagoya 466-8550, Aichi, Japan.

**E-mail:** [kasuya@med.nagoya-u.ac.jp](mailto:kasuya@med.nagoya-u.ac.jp)



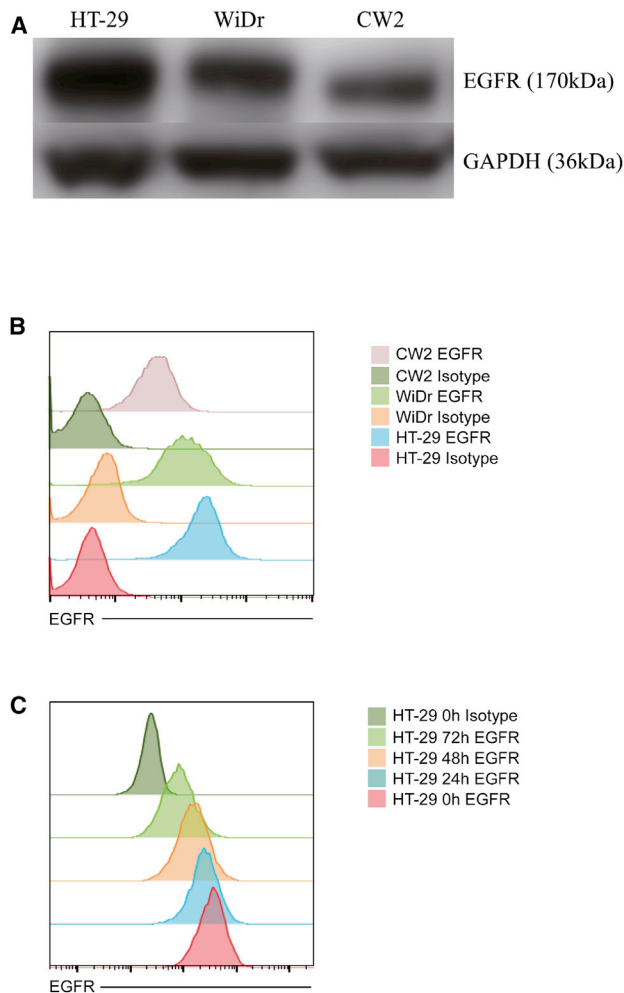


**Figure 1. Evaluation of EGFR Expression**

(A and B) EGFR expression in three human colorectal cancer cell lines (HT-29, WiDr, and CW2) was measured by western blotting (A) and flow cytometry (B). (C) EGFR expression in HT-29 was detected by flow cytometry after C-REV infection. GAPDH was used as the endogenous control.

antiangiogenic effect by decreasing VEGF production.<sup>22</sup> Moreover, cetuximab can induce antibody-dependent cellular cytotoxicity (ADCC) through Fc $\gamma$  receptors on immune effector cells, such as natural killer (NK) cells and macrophages. In CRC, cetuximab-mediated ADCC activity is correlated with the expression of EGFR.<sup>23,24</sup>

In this study, we combined C-REV and cetuximab to treat human CRC, and we evaluated the antitumor efficacy of this regimen. Cetuximab treatment prior to C-REV treatment strongly inhibited tumor growth by enhancing virus spread and preventing angiogenesis.

## RESULTS

### EGFR Expression Level in CRC Cell Lines

We compared the expression level of EGFR among three CRC cell lines, HT-29, WiDr, and CW2, by western blotting and flow

cytometry (Figures 1A and 1B). HT-29 expressed the highest level of EGFR and CW2 the lowest. To determine whether C-REV treatment affects EGFR expression, we performed flow cytometry to detect EGFR after C-REV infection. In our flow cytometry analysis, dead cells after C-REV treatment were eliminated by gating of forward scatter and side scatter. Only living cells were detected and recorded. EGFR expression of all three cell lines was reduced 3 days after C-REV (MOI 1) infection (Figure 1C; Figure S1). This result suggested that C-REV infection directly modulates EGFR expression in CRC cell lines.

### Cytotoxicity of Cetuximab and C-REV in CRC Cell Lines and Cetuximab Has No Effect on Viral Replication

Because the expression of EGFR differed among the CRC cell lines, we used the 3-(4,5-dimethylthiazol-2-yl)-2,5-diphenyl tetrazolium bromide (MTT) assay to evaluate the sensitivity of HT-29, WiDr, and CW2 to C-REV, cetuximab, and their combination. C-REV exerted a strong cytotoxic effect on all three cell lines, and its effect was time- and dose- dependent. Cetuximab alone had a slightly cytotoxic effect *in vitro* (Figure 2A), and combination therapy with cetuximab and C-REV had no additive effect (Figure 2B).

To determine whether cetuximab affects viral replication in CRC cell lines, we titrated virus from infected cells in order to assess viral replication. We infected three cell lines with C-REV (MOI 1), and we co-incubated them with various concentrations of cetuximab (5, 10, and 20  $\mu$ g/mL) for 3 days. Cetuximab had no effect on viral replication in any of the three cell lines (Figure 2C).

### Combination Therapy with Cetuximab and C-REV Exerts a Strong Antitumor Effect in HT-29 Tumor Xenografts

Next, we evaluated the *in vivo* antitumor efficacy of combination therapy with cetuximab and C-REV. To determine combination therapy with cetuximab and C-REV, we chose HT-29 tumor xenografts, as HT-29 expressed the highest level of EGFR among the cell lines we examined. We applied two kinds of treatment regimens to our tumor model (Figures 3A and 3D), and we compared their efficacy. C-REV was injected intratumorally at the same time in both regimens (days 1, 4, and 7), and cetuximab was injected intraperitoneally prior to (combination G1) or after C-REV (combination G2).

Combination G1 suppressed tumor growth significantly relative to either single therapy (Figure 3B); combination G2 was superior to the control and cetuximab groups, but it was not significantly different from the C-REV group (Figure 4E). Based on measurement of fractional tumor volume (FTV), combination G1 synergistically inhibited tumor growth (Table 1). No adverse effects were observed in the tumor model, as assessed by the evaluation of body weight (Figure 3C).

### Antiangiogenic Effect Is Enhanced Significantly in Combination Therapy

C-REV promotes tumor angiogenesis, whereas erlotinib, an EGFR kinase inhibitor, decreases this effect.<sup>20</sup> Hence, we investigated tumor

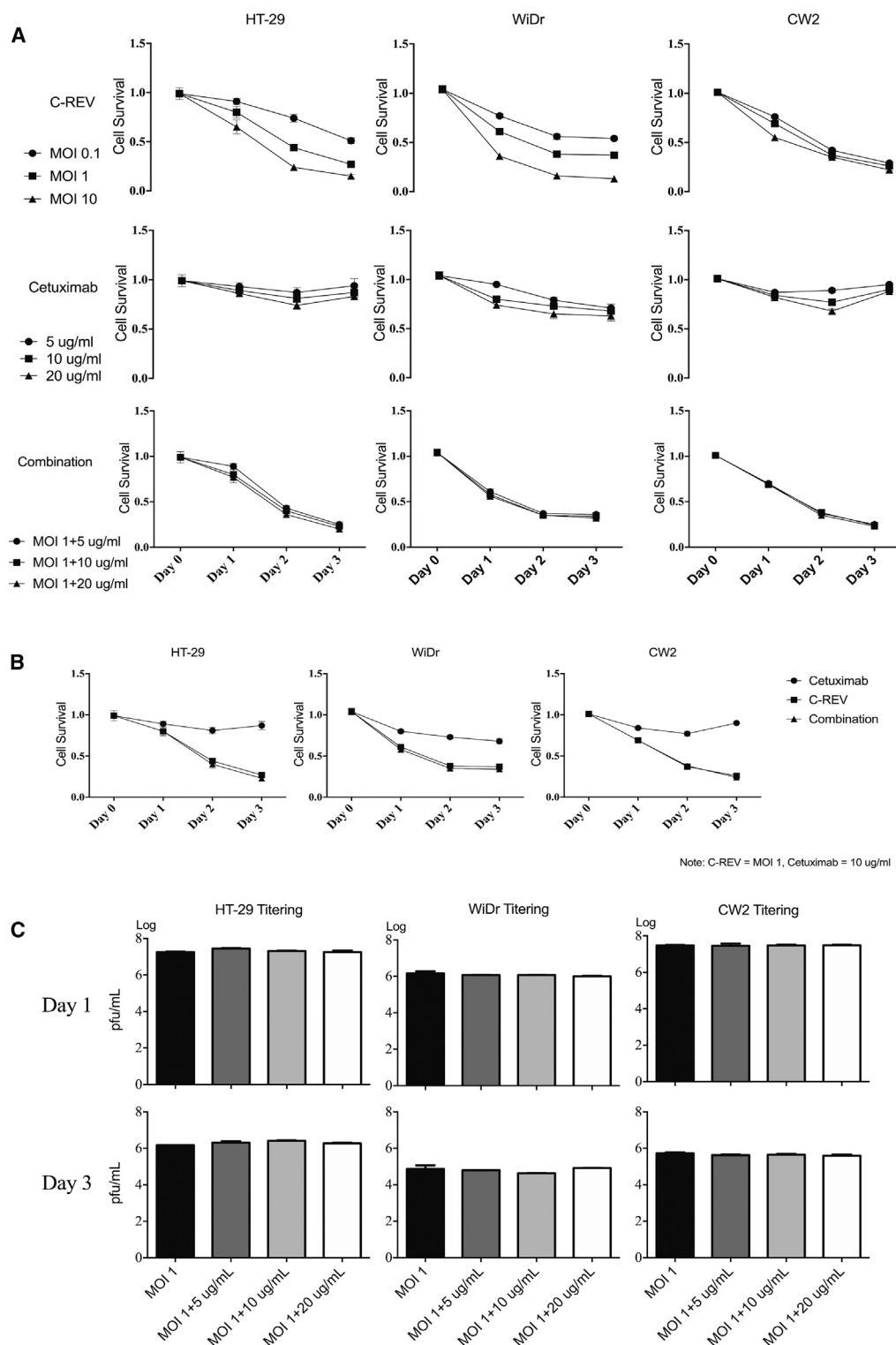


**Figure 2. Viral Cytotoxicity Assay and Viral Titering**

(A) *In vitro* sensitivity to C-REV, cetuximab, and their combination in HT-29, WiDr, and CW2 cells, as determined by MTT assay. The results are shown as means  $\pm$  SD. (B) Comparison of cytotoxicity for three kinds of treatments (C-REV, cetuximab, and combination) in each cell line, as determined by MTT assay. (C) *In vitro* replication of C-REV (MOI 1) over a 3-day period, co-incubated with doses equivalent to 5, 10, or 20  $\mu$ g/mL cetuximab, as assessed by viral titer.

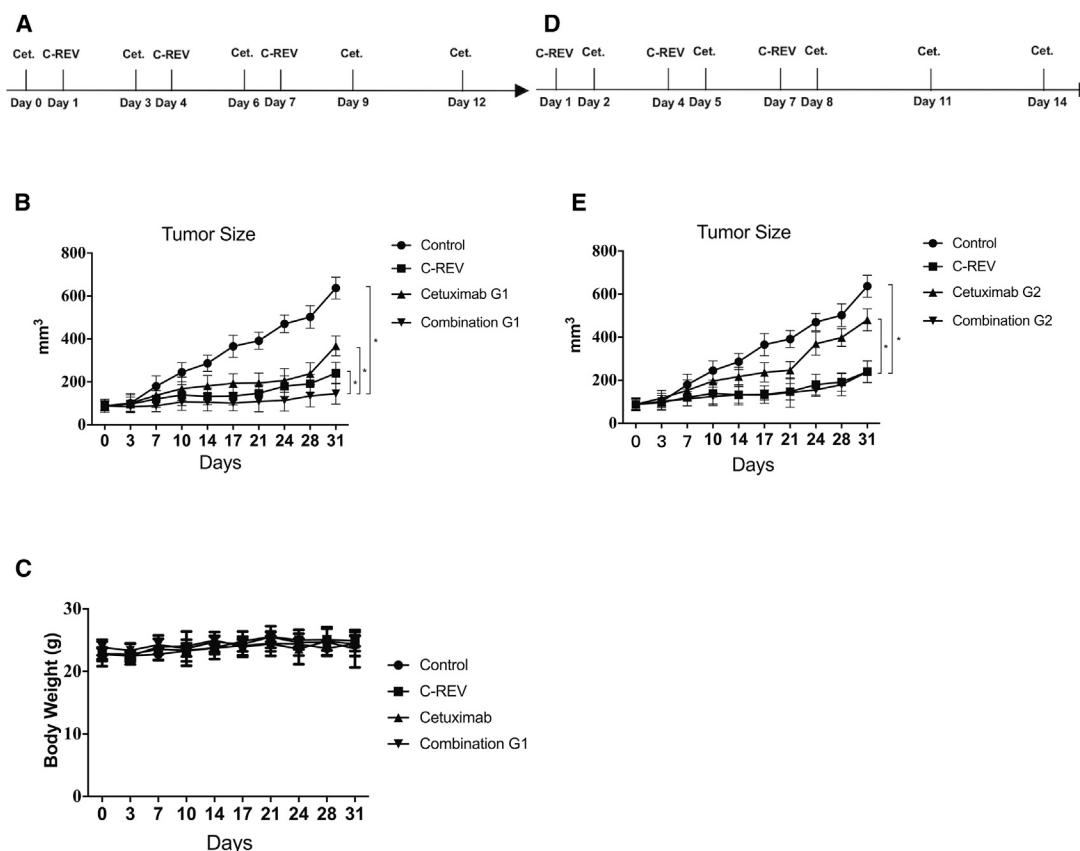


**Figure 3. Antitumor Effects of Cetuximab and C-REV in HT-29 Tumor Xenografts**

HT-29 cells were inoculated into 5- to 6-week-old male BALB/c nude mice. The mice were treated with C-REV ( $5 \times 10^6$  PFU) and cetuximab (0.25 mg) and followed up twice a week for tumor growth. (A) Treatment protocol for the tumor model of human colorectal cancer xenografts. Cetuximab was applied first, followed by an injection of C-REV. Day 0 is the start of cetuximab treatment. (B) Tumor size in each treatment group of the human colorectal cancer xenograft model, as followed by the protocol in (A). \* $p < 0.001$ . (C) Body weight in the human colorectal cancer xenograft model. (D) The other administration order for the human colorectal cancer xenograft model: C-REV was injected prior to cetuximab administration. C-REV injection was performed on the same day in both therapy schedules. (E) Tumor size in each treatment group of the human colorectal cancer xenograft model, as followed by the protocol in (D). \* $p < 0.001$ . Data are presented as means  $\pm$  SD, and statistical differences between groups were evaluated by one-way ANOVA. Only significant differences are indicated.

angiogenesis after treatment with C-REV and cetuximab. Tumor samples were collected on day 3 (2 days after the last C-REV injection) and day 14 (13 days after the last C-REV injection), and immunohistochemical staining of HSV and CD31 were performed to evaluate virus distribution and neovascularization.

HSV-1 virus distribution within the tumor was enhanced in the combination G1 group relative to the C-REV group on day 3 (Figures 4A and 4B). Cetuximab suppressed angiogenesis (CD31-positive spots, arrows) relative to the control and C-REV groups. Cetuximab also enhanced the antiangiogenic effect on day 14 in the combination G1 group relative to the C-REV group (Figure 4C). Meanwhile, both CD31 staining and microvessel density (MVD) revealed that the antiangiogenic effect was significantly enhanced in combination G1 relative to combination G2 (Figures 4C and 4D). The antiangiogenic effect was consistent with the *in vivo* antitumor effect of combination therapy.

## DISCUSSION

In this study, we evaluated the effect of combination therapy with cetuximab and the oncolytic herpes virus C-REV on human CRC cell lines and tumor xenografts. Cell viability assays revealed that the cytotoxicity of C-REV was time and dose dependent (Figure 2A). Viral replication assays indicated that cetuximab did not interfere with viral replication at any dose, implying that viral replication was not affected by inhibition of the EGFR pathway *in vitro* (Figure 2C). Combination therapy with cetuximab and C-REV suppressed tumor growth significantly relative to other treatments (Figure 3B). HSV-1 staining revealed that the virus was distributed more efficiently in the combination therapy group than in the C-REV group (Figure 4A). Injection of C-REV prior to cetuximab had no additive effect on tumor growth relative to C-REV treatment alone (Figure 3E).

Preclinical studies and clinical trials over the past decades have shown that oncolytic viruses have potential efficacy against various tumors,

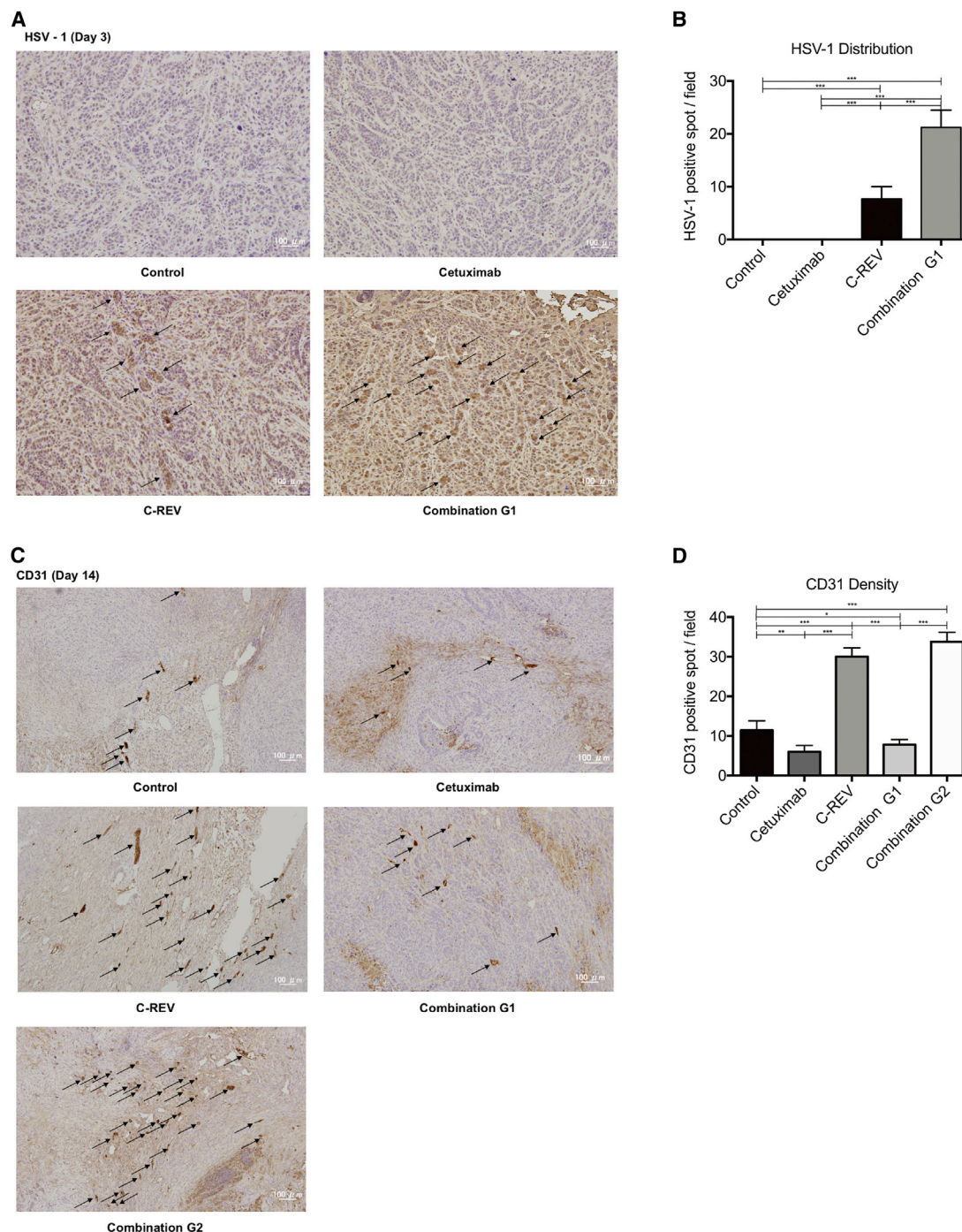


**Figure 4. Immunohistochemical Staining of Tumor Samples**

(A) Immunohistochemical staining of HSV-1 (arrows) in tumors from the C-REV group and combination G1 group, 3 days post-treatment (200 $\times$  magnification; scale bars, 100  $\mu$ m). (B) Quantitative analysis of the results in (A). HSV-1 density in the tumor was assessed at 200 $\times$  magnification. (C) Immunohistochemical staining for CD31 (arrows) in tumors from the control group, cetuximab group, C-REV group, combination G1 group, and combination G2 group, 14 days post-treatment (100 $\times$  magnification; scale bars, 100  $\mu$ m). (D) Quantitative analysis of the results of (C). CD31 density in tumors was assessed at 100 $\times$  magnification. Data are presented as means  $\pm$  SD, and statistical differences between groups were evaluated by one-way ANOVA. \* $p$  < 0.05, \*\* $p$  < 0.01, \*\*\* $p$  < 0.001. Only significant differences are indicated.

**Table 1. Fractional Tumor Volume (FTV) following Treatment with Cetuximab and C-REV, Alone or in Combination, in HT-29 Tumor Xenografts**

Day	C-REV	Cetuximab	Combination G1		
			E-FTV	O-FTV	E-FTV/O-FTV <sup>a</sup>
7	0.66975	0.76355	0.51139	0.49087	1.04180
10	0.56577	0.71399	0.40396	0.36818	1.09720
14	0.52165	0.69182	0.36089	0.32420	1.11316
17	0.47963	0.61112	0.29311	0.25897	1.13184
21	0.50240	0.62543	0.31422	0.24809	1.26655
24	0.45649	0.60908	0.27804	0.21237	1.30922
28	0.45490	0.61450	0.27953	0.20818	1.34275
31	0.45579	0.57689	0.26295	0.18046	1.45709

FTV, fractional tumor volume (mean tumor volume experimental/mean tumor volume control); E-FTV, expected FTV (mean FTV of C-REV)  $\times$  (mean FTV of cetuximab); O-FTV, observed FTV.

<sup>a</sup>Synergic effect: E-FTV/O-FTV > 1.

but the inefficient distribution capability of virus in tumors always limited clinical efficacy.<sup>25–27</sup> Oncolytic virus distribution is highly affected by the tumor microenvironment.<sup>28</sup> High levels of secretion of extracellular matrix proteins by tumor cells contribute to high interstitial fluid pressure (IFP), which is one of the major factors preventing viruses from spreading in tumors.<sup>28</sup> Because IFP increases as the tumor grows, the tumor angiogenesis is closely linked to high IFP.<sup>29–31</sup> Therefore, antiangiogenic therapy has been proposed as a means to promote more efficient viral distribution. In our previous studies, we reported that bevacizumab and erlotinib, via their antiangiogenic effects, enhanced the distribution of the oncolytic herpes virus C-REV in human breast cancer xenografts and pancreatic cancer xenografts, respectively.<sup>20,32</sup>

Inhibition of EGFR by tyrosine kinase inhibitors or monoclonal antibodies decreases the angiogenic profile of tumor cells,<sup>33</sup> whereas overexpression of EGFR on tumor cells is related to the production of angiogenic molecules. Bruns et al.<sup>34</sup> reported that cetuximab decreased the production of VEGF and interleukin (IL)-8 in pancreatic cancer *in vitro* and *in vivo*. Cetuximab also reduced VEGF, basic fibroblast growth factor (bFGF), and transforming growth factor  $\alpha$  (TGF- $\alpha$ ) expressions and decreased microvessel count in CRC cells and xenografts.<sup>35</sup> Together, these findings indicated that cetuximab has an antiangiogenic effect. In this study, immunohistochemical staining for CD31 revealed that the combination of cetuximab and C-REV decreased tumor angiogenesis relative to C-REV treatment alone (Figures 4C and 4D). HSV can induce angiogenesis in various tumors,<sup>17,18,36</sup> and viral infection induces the production of VEGF.<sup>37–42</sup> Hence, the inhibition of angiogenesis by cetuximab improved the antitumor effect of C-REV in the HT-29 xenograft model by promoting efficient virus distribution within the tumor.

In addition, the decrease in EGFR expression after treatment with C-REV is related to the therapeutic effects of cetuximab. Liang et al.<sup>43</sup>

demonstrated that HSV-1 ICP0 can interact with CIN85 and Cbl, forming a complex that downregulates cell surface levels of EGFR in the absence of EGF. Their result is in accordance with our finding that the expression of EGFR on three CRC cell lines decreased following C-REV infection (Figure 1C; Figure S1). This result may explain that C-REV prior to cetuximab combination therapy had no additive inhibitory effect relative to the C-REV group. Moreover, C-REV-induced angiogenesis was not inhibited by cetuximab *in vivo* (Figure 4C, combination G2). However, other researchers reported that the interaction between EGFR and PI3K was upregulated and EGFR was transiently activated during HSV-1 infection.<sup>44</sup> We also determined that the expression of EGFR *in vitro* was temporarily increased after C-REV administration but subsequently decreased (Figure S2). Further studies are needed to explore the internal mechanism underlying this finding.

Our results show that the combination of the anti-EGFR monoclonal antibody cetuximab and the oncolytic virus C-REV induced a synergistic antitumor effect in a human CRC xenograft model. Cetuximab enhanced the antitumor activity of C-REV by promoting viral distribution and inhibiting angiogenesis. Therefore, cetuximab represents an ideal virus-associated agent for antitumor therapy. Our findings suggest that applying cetuximab prior to C-REV can gain more benefit in tumor growth inhibition. With further investigation, combination therapy could be developed into an effective antitumor strategy against human CRC.

## MATERIALS AND METHODS

### Cell Lines and Viruses

The human CRC cell line WiDr and African green monkey kidney cell line Vero were obtained from American Type Culture Collection (Manassas, VA, USA). The human CRC cell line CW2 was obtained from the RIKEN Cell Bank (Tsukuba, Japan). The human CRC cell line HT-29 was kindly donated by Dr. Suguru Yamada (Nagoya University, Japan). HT-29, WiDr, CW2, and Vero cells were grown in DMEM (Sigma, Tokyo, Japan) supplemented with 10% fetal calf serum (FCS) and 1% penicillin/streptomycin (Gibco). C-REV is a highly attenuated mutant clone derived from HSV-1 strain HF.<sup>45</sup> The virus was propagated in Vero cells and stored in aliquots at  $-80^{\circ}\text{C}$ . C-REV was diluted in PBS for *in vivo* and *in vitro* experiments. Viral titers were assayed in Vero cells and expressed as plaque-forming units per milliliter (PFU/mL).

### Western Blot

Proteins were separated by electrophoresis and then transferred to polyvinylidene fluoride (PVDF) membranes using an iBlot apparatus (Invitrogen, MA). After blocking in skim milk for 1 h, the membrane was washed with TBS with Tween 20 (TBS-T) buffer at room temperature (RT). Primary antibodies against EGFR (Abcam, Cambridge, UK) and glyceraldehyde-3-phosphate dehydrogenase (GAPDH; Abcam) were added, and the membranes were shaken gently for 1 h at RT. After three washes with TBS-T, the membranes were incubated with horseradish peroxidase (HRP)-labeled secondary antibody (anti-rabbit immunoglobulin G [IgG]) for 1 h at RT, and then they

were washed three times in TBS-T. Immunoreactive bands of proteins were visualized using the ECL Plus Solution (Amersham, Arlington Heights, IL, USA), and signals were recorded by autoradiography.

### Cell Viability

Cell proliferation was evaluated using the MTT dye reduction method as described.<sup>46,47</sup> Tumor cells were seeded in 96-well plates (5,000 cells/well) and incubated with DMEM (supplemented with 10% FCS and 1% penicillin/streptomycin) at 37°C and 5% CO<sub>2</sub>. After 24 h, cells were exposed to serial dilutions of cetuximab (Merck Serono, Germany) and/or C-REV at the indicated MOIs. The day of treatment was designated as day 0. Cells were grown for another 1, 2, or 3 days. Viable cells were quantified using colorimetric MTT assays.

### Viral Proliferation Assay

Cells were placed on six-well plates and incubated overnight. The following day, the cells were treated with C-REV at an MOI of 1 and incubated with various concentrations of cetuximab (5, 10, and 20 µg/mL). Then, 3 days later, cells were scraped, and the supernatants were collected and subjected to three freeze-thaw cycles. The released virus particles were collected and serially diluted in DMEM without fetal bovine serum (FBS). Following a standard viral plaque assay,<sup>48,49</sup> Vero cells were infected with serial dilutions of viruses in 6-well plates for 1 h. The viral supernatant was removed and 2% low-melting agarose was added. Cells were incubated at 37°C for 5–7 days until the plaques could be counted.

### Determination of EGFR Expression Level by Flow Cytometry

All three CRC cell lines were treated with or without C-REV; infections ran for 3 days. Cells were collected on days 1, 2, and 3 and stained with isotype control antibody (allophycocyanin [APC]) (eBioscience) and anti-human EGFR antibody (APC) (BioLegend) at 4°C for 10 min. Stained cells were washed twice with fluorescence-activated cell sorting (FACS) buffer and fixed in 4% paraformaldehyde. Data were acquired on a FACSCanto II (BD Biosciences) and analyzed using the FlowJo software.

### Animal Studies

The 5- to 6-week-old male BALB/c Slc-nu/nu mice were obtained from Japan SLC (Shizuoka, Japan). All animal experiments were conducted in accordance with the guidelines issued by the Nagoya University Animal Center. Suspensions of HT-29 tumor cells ( $5 \times 10^6$  cells/100 µL) were subcutaneously injected into the backs of the mice. Tumors were allowed to reach a volume of about 100 mm<sup>3</sup>. The mice were then randomly divided into six groups of 10: control, cetuximab (G1 and G2), C-REV, and combination of cetuximab and C-REV (G1 and G2).

Mice in the C-REV group and combination group (G1 and G2) were treated with C-REV ( $5 \times 10^6$  PFU/50 µL intratumorally [i.t.]) every 3 days for 1 week. Mice in the cetuximab group (G1 and G2) and combination group (G1 and G2) were treated with cetuximab (0.25 mg/injection intraperitoneally [i.p.]) every 3 days for 2 weeks. Cetuximab was injected 24 h before or after C-REV injection. The first

day of C-REV treatment was designated as day 1. Cetuximab was administered 24 h before or after the first dose of C-REV. Tumor size and body weight were measured twice a week.

Tumor volume (V) was evaluated using the equation  $V = LW^2/2$ , where L and W were tumor length and width, respectively. To determine the presence or absence of synergy between cetuximab and C-REV, we used the FTV method.<sup>50,51</sup> Here, the expected FTV of the combination treatment was divided by the observed FTV of the combination treatment, yielding a ratio that indicated the interaction (>1 indicates synergy and <1 a less than additive effect). FTV for each treatment group was obtained by dividing the mean tumor volume of the treatment group by that of the control group.

In a separate experiment, mice bearing subcutaneous HT-29-derived tumors were randomly divided into six groups of three to receive treatment. On days 3 and 14 (2 days and 13 days after the last C-REV injection), tumor samples were collected for immunohistochemical staining.

### Immunohistochemistry

Tumors samples were fixed and embedded in paraffin, and then they were sectioned at a 5-µm thickness to prepare slides for immunohistochemical staining. HSV-1 and CD31 were detected using anti-HSV-1 antibody (1/100 dilution; Imgenex, CA, USA) and anti-CD31 antibody (1/50 dilution; Abcam), respectively. Antigen retrieval was performed by autoclaving for 15 min in Tris-EDTA (pH 9.0). After blocking with 3% normal goat serum (Histofine; Nichirei Biosciences, Tokyo, Japan), sections were incubated overnight with the primary antibodies described above. Biotinylated anti-rabbit IgG (Histofine; Nichirei Biosciences) was used as the secondary antibody. HRP-3,3'-diaminobenzidine (Histofine; Nichirei Biosciences) was used as the chromogenic agent. Each slide was examined by microscopy at 100× magnification. Five random fields of view in each section were chosen for histological quantification. CD31 density was evaluated by counting the number of CD31-stained microvessels within these areas.

### Statistical Analysis

Continuous variables were compared with ANOVA. Differences were considered to be statistically significant when p values were less than 0.05. All analyses were conducted using the Prism 7 software (GraphPad, San Diego, CA, USA).

### SUPPLEMENTAL INFORMATION

Supplemental Information can be found online at <https://doi.org/10.1016/j.omto.2019.04.004>.

### AUTHOR CONTRIBUTIONS

Z.W. performed primary preparation of the manuscript, data collection, design, writing, and editing. T.I. performed manuscript writing, data collection, and editing. Y. Naoe performed revision of the manuscript, with critical considerations regarding manuscript design and editing. I.B.V., S.M., and M.T. revised the manuscript. I.R.E., S.Y.,

N. Miyajima, D.M., N. Mukoyama, Y. Nishikawa, and Y. Koide performed manuscript design and data collection. Y. Kodera and H.K. performed revision of the manuscript, with critical considerations regarding manuscript design, as well as final approval of the version to be published.

## CONFLICTS OF INTEREST

M.T. is an employee of Takara Bio Inc. The other authors declare no competing interests.

## ACKNOWLEDGMENTS

We appreciate professor Yukihiro Nishiyama for his valuable suggestions and Emi Uematsu and Yumiko Samizo for their great support. This study was financially supported by Japan Grant-in-Aid for Scientific Research 2016 (JP16H05413).

## REFERENCES

1. Ferlay, J., Soerjomataram, I., Dikshit, R., Eser, S., Mathers, C., Rebelo, M., Parkin, D.M., Forman, D., and Bray, F. (2015). Cancer incidence and mortality worldwide: sources, methods and major patterns in GLOBOCAN 2012. *Int. J. Cancer* 136, E359–E386.
2. Katanoda, K., Matsuda, T., Matsuda, A., Shibata, A., Nishino, Y., Fujita, M., Soda, M., Ioka, A., Sobue, T., and Nishimoto, H. (2013). An updated report of the trends in cancer incidence and mortality in Japan. *Jpn. J. Clin. Oncol.* 43, 492–507.
3. Arnold, M., Sierra, M.S., Laversanne, M., Soerjomataram, I., Jemal, A., and Bray, F. (2017). Global patterns and trends in colorectal cancer incidence and mortality. *Gut* 66, 683–691.
4. Brenner, H., Kloor, M., and Pox, C.P. (2014). Colorectal cancer. *Lancet* 383, 1490–1502.
5. Miest, T.S., and Cattaneo, R. (2014). New viruses for cancer therapy: meeting clinical needs. *Nat. Rev. Microbiol.* 12, 23–34.
6. Kaufman, H.L., Kohlhaas, F.J., and Zloza, A. (2015). Oncolytic viruses: a new class of immunotherapy drugs. *Nat. Rev. Drug Discov.* 14, 642–662.
7. Greig, S.L. (2016). Talimogene Laherparepvec: First Global Approval. *Drugs* 76, 147–154.
8. Fujimoto, Y., Mizuno, T., Sugiura, S., Goshima, F., Kohno, S., Nakashima, T., and Nishiyama, Y. (2006). Intratumoral injection of herpes simplex virus HF10 in recurrent head and neck squamous cell carcinoma. *Acta Otolaryngol.* 126, 1115–1117.
9. Hirooka, Y., Kasuya, H., Ishikawa, T., Kawashima, H., Ohno, E., Villalobos, I.B., Naoe, Y., Ichinose, T., Koyama, N., Tanaka, M., et al. (2018). A Phase I clinical trial of EUS-guided intratumoral injection of the oncolytic virus, HF10 for unresectable locally advanced pancreatic cancer. *BMC Cancer* 18, 596.
10. Hotta, Y., Kasuya, H., Bustos, I., Naoe, Y., Ichinose, T., Tanaka, M., and Kodera, Y. (2017). Curative effect of HF10 on liver and peritoneal metastasis mediated by host antitumor immunity. *Oncolytic Virother.* 6, 31–38.
11. Kasuya, H., Kodera, Y., Nakao, A., Yamamura, K., Gewen, T., Zhiwen, W., Hotta, Y., Yamada, S., Fujii, T., Fukuda, S., et al. (2014). Phase I Dose-escalation Clinical Trial of HF10 Oncolytic Herpes Virus in 17 Japanese Patients with Advanced Cancer. *Hepatogastroenterology* 61, 599–605.
12. Kimata, H., Imai, T., Kikumori, T., Teshigahara, O., Nagasaka, T., Goshima, F., Nishiyama, Y., and Nakao, A. (2006). Pilot study of oncolytic viral therapy using mutant herpes simplex virus (HF10) against recurrent metastatic breast cancer. *Ann. Surg. Oncol.* 13, 1078–1084.
13. Kohno, S., Luo, C., Goshima, F., Nishiyama, Y., Sata, T., and Ono, Y. (2005). Herpes simplex virus type 1 mutant HF10 oncolytic viral therapy for bladder cancer. *Urology* 66, 1116–1121.
14. Nakao, A., Kasuya, H., Sahin, T.T., Nomura, N., Kanzaki, A., Misawa, M., Shiota, T., Yamada, S., Fujii, T., Sugimoto, H., et al. (2011). A phase I dose-escalation clinical trial of intraoperative direct intratumoral injection of HF10 oncolytic virus in non-resectable patients with advanced pancreatic cancer. *Cancer Gene Ther.* 18, 167–175.
15. Nakao, A., Takeda, S., Shimoyama, S., Kasuya, H., Kimata, H., Teshigahara, O., Sawaki, M., Kikumori, T., Kodera, Y., Nagasaka, T., et al. (2007). Clinical experiment of mutant herpes simplex virus HF10 therapy for cancer. *Curr. Cancer Drug Targets* 7, 169–174.
16. Sahin, T.T., Kasuya, H., Nomura, N., Shikano, T., Yamamura, K., Gewen, T., Kanzaki, A., Fujii, T., Sugae, T., Imai, T., et al. (2012). Impact of novel oncolytic virus HF10 on cellular components of the tumor microenvironment in patients with recurrent breast cancer. *Cancer Gene Ther.* 19, 229–237.
17. Aghi, M., Rabkin, S.D., and Martuza, R.L. (2007). Angiogenic response caused by oncolytic herpes simplex virus-induced reduced thrombospondin expression can be prevented by specific viral mutations or by administering a thrombospondin-derived peptide. *Cancer Res.* 67, 440–444.
18. Kurozumi, K., Hardcastle, J., Thakur, R., Shroll, J., Nowicki, M., Otsuki, A., Chiocca, E.A., and Kaur, B. (2008). Oncolytic HSV-1 infection of tumors induces angiogenesis and upregulates CYR61. *Mol. Ther.* 16, 1382–1391.
19. Bareschino, M.A., Schettino, C., Troiani, T., Martinelli, E., Morgillo, F., and Ciardiello, F. (2007). Erlotinib in cancer treatment. *Ann. Oncol.* 18 (Suppl 6), vi35–vi41.
20. Yamamura, K., Kasuya, H., Sahin, T.T., Tan, G., Hotta, Y., Tsurumaru, N., Fukuda, S., Kanda, M., Kobayashi, D., Tanaka, C., et al. (2014). Combination treatment of human pancreatic cancer xenograft models with the epidermal growth factor receptor tyrosine kinase inhibitor erlotinib and oncolytic herpes simplex virus HF10. *Ann. Surg. Oncol.* 21, 691–698.
21. Salomon, D.S., Brandt, R., Ciardiello, F., and Normanno, N. (1995). Epidermal growth factor-related peptides and their receptors in human malignancies. *Crit. Rev. Oncol. Hematol.* 19, 183–232.
22. Okada, Y., Miyamoto, H., Goji, T., and Takayama, T. (2014). Biomarkers for predicting the efficacy of anti-epidermal growth factor receptor antibody in the treatment of colorectal cancer. *Digestion* 89, 18–23.
23. Correale, P., Marra, M., Remondo, C., Migali, C., Misso, G., Arcuri, F.P., Del Vecchio, M.T., Carducci, A., Loiacono, L., Tassone, P., et al. (2010). Cytotoxic drugs up-regulate epidermal growth factor receptor (EGFR) expression in colon cancer cells and enhance their susceptibility to EGFR-targeted antibody-dependent cell-mediated cytotoxicity (ADCC). *Eur. J. Cancer* 46, 1703–1711.
24. Seo, Y., Ishii, Y., Ochiai, H., Fukuda, K., Akimoto, S., Hayashida, T., Okabayashi, K., Tsuruta, M., Hasegawa, H., and Kitagawa, Y. (2014). Cetuximab-mediated ADCC activity is correlated with the cell surface expression level of EGFR but not with the KRAS/BRAF mutational status in colorectal cancer. *Oncol. Rep.* 31, 2115–2122.
25. Nemunaitis, J., Khuri, F., Ganly, I., Arseneau, J., Posner, M., Vokes, E., Kuhn, J., McCarty, T., Landers, S., Blackburn, A., et al. (2001). Phase II trial of intratumoral administration of ONYX-015, a replication-selective adenovirus, in patients with refractory head and neck cancer. *J. Clin. Oncol.* 19, 289–298.
26. Parato, K.A., Senger, D., Forsyth, P.A., and Bell, J.C. (2005). Recent progress in the battle between oncolytic viruses and tumours. *Nat. Rev. Cancer* 5, 965–976.
27. Liu, T.C., Galanis, E., and Kirn, D. (2007). Clinical trial results with oncolytic virotherapy: a century of promise, a decade of progress. *Nat. Clin. Pract. Oncol.* 4, 101–117.
28. Wojton, J., and Kaur, B. (2010). Impact of tumor microenvironment on oncolytic viral therapy. *Cytokine Growth Factor Rev.* 21, 127–134.
29. Boucher, Y., Leunig, M., and Jain, R.K. (1996). Tumor angiogenesis and interstitial hypertension. *Cancer Res.* 56, 4264–4266.
30. Boucher, Y., and Jain, R.K. (1992). Microvascular pressure is the principal driving force for interstitial hypertension in solid tumors: implications for vascular collapse. *Cancer Res.* 52, 5110–5114.
31. Heldin, C.H., Rubin, K., Pietras, K., and Ostman, A. (2004). High interstitial fluid pressure - an obstacle in cancer therapy. *Nat. Rev. Cancer* 4, 806–813.
32. Tan, G., Kasuya, H., Sahin, T.T., Yamamura, K., Wu, Z., Koide, Y., Hotta, Y., Shikano, T., Yamada, S., Kanzaki, A., et al. (2015). Combination therapy of oncolytic herpes simplex virus HF10 and bevacizumab against experimental model of human breast carcinoma xenograft. *Int. J. Cancer* 136, 1718–1730.

33. van Cruysen, H., Giaccone, G., and Hoekman, K. (2005). Epidermal growth factor receptor and angiogenesis: Opportunities for combined anticancer strategies. *Int. J. Cancer* 117, 883–888.
34. Bruns, C.J., Harbison, M.T., Davis, D.W., Portera, C.A., Tsan, R., McConkey, D.J., Evans, D.B., Abbruzzese, J.L., Hicklin, D.J., and Radinsky, R. (2000). Epidermal growth factor receptor blockade with C225 plus gemcitabine results in regression of human pancreatic carcinoma growing orthotopically in nude mice by antiangiogenic mechanisms. *Clin. Cancer Res.* 6, 1936–1948.
35. Ciardiello, F., Bianco, R., Damiano, V., Fontanini, G., Caputo, R., Pomato, G., De Placido, S., Bianco, A.R., Mendelsohn, J., and Tortora, G. (2000). Antiangiogenic and antitumor activity of anti-epidermal growth factor receptor C225 monoclonal antibody in combination with vascular endothelial growth factor antisense oligonucleotide in human GEO colon cancer cells. *Clin. Cancer Res.* 6, 3739–3747.
36. Hardcastle, J., Kurozumi, K., Dmitrieva, N., Sayers, M.P., Ahmad, S., Waterman, P., Weissleder, R., Chiocca, E.A., and Kaur, B. (2010). Enhanced antitumor efficacy of vasculostatin (Vstat120) expressing oncolytic HSV-1. *Mol. Ther.* 18, 285–294.
37. Boshoff, C. (1998). Kaposi's sarcoma. Coupling herpesvirus to angiogenesis. *Nature* 391, 24–25.
38. Zheng, M., Schwarz, M.A., Lee, S., Kumaraguru, U., and Rouse, B.T. (2001). Control of stromal keratitis by inhibition of neovascularization. *Am. J. Pathol.* 159, 1021–1029.
39. Zheng, M., Klinman, D.M., Gierynska, M., and Rouse, B.T. (2002). DNA containing CpG motifs induces angiogenesis. *Proc. Natl. Acad. Sci. USA* 99, 8944–8949.
40. Hayashi, K., Hooper, L.C., Detrick, B., and Hooks, J.J. (2009). HSV immune complex (HSV-IgG: IC) and HSV-DNA elicit the production of angiogenic factor VEGF and MMP-9. *Arch. Virol.* 154, 219–226.
41. Wuest, T.R., and Carr, D.J. (2010). VEGF-A expression by HSV-1-infected cells drives corneal lymphangiogenesis. *J. Exp. Med.* 207, 101–115.
42. Currier, M.A., Eshun, F.K., Sholl, A., Chernoguz, A., Crawford, K., Divanovic, S., Boon, L., Goins, W.F., Frischer, J.S., Collins, M.H., et al. (2013). VEGF blockade enables oncolytic cancer virotherapy in part by modulating intratumoral myeloid cells. *Mol. Ther.* 21, 1014–1023.
43. Liang, Y., Kurakin, A., and Roizman, B. (2005). Herpes simplex virus 1 infected cell protein 0 forms a complex with CIN85 and Cbl and mediates the degradation of EGF receptor from cell surfaces. *Proc. Natl. Acad. Sci. USA* 102, 5838–5843.
44. Zheng, K., Xiang, Y., Wang, X., Wang, Q., Zhong, M., Wang, S., Wang, X., Fan, J., Kitazato, K., and Wang, Y. (2014). Epidermal growth factor receptor-PI3K signaling controls cofilin activity to facilitate herpes simplex virus 1 entry into neuronal cells. *MBio* 5, e00958-13.
45. Nishiyama, Y., Kimura, H., and Daikoku, T. (1991). Complementary lethal invasion of the central nervous system by nonneuroinvasive herpes simplex virus types 1 and 2. *J. Virol.* 65, 4520–4524.
46. Carroll, N.M., Chiocca, E.A., Takahashi, K., and Tanabe, K.K. (1996). Enhancement of gene therapy specificity for diffuse colon carcinoma liver metastases with recombinant herpes simplex virus. *Ann. Surg.* 224, 323–329, discussion 329–330.
47. Kasuya, H., Pawlik, T.M., Mullen, J.T., Donahue, J.M., Nakamura, H., Chandrasekhar, S., Kawasaki, H., Choi, E., and Tanabe, K.K. (2004). Selectivity of an oncolytic herpes simplex virus for cells expressing the DF3/MUC1 antigen. *Cancer Res.* 64, 2561–2567.
48. Cooper, L.A., Sina, B.J., Turell, M.J., and Scott, T.W. (2000). Effects of initial dose on eastern equine encephalomyelitis virus dependent mortality in intrathoracically inoculated *Culiseta melanura* (Diptera: Culicidae). *J. Med. Entomol.* 37, 815–819.
49. LaBarre, D.D., and Lowy, R.J. (2001). Improvements in methods for calculating virus titer estimates from TCID<sub>50</sub> and plaque assays. *J. Virol. Methods* 96, 107–126.
50. Yokoyama, Y., Dhanabal, M., Griffioen, A.W., Sukhatme, V.P., and Ramakrishnan, S. (2000). Synergy between angiostatin and endostatin: inhibition of ovarian cancer growth. *Cancer Res.* 60, 2190–2196.
51. Yu, D.C., Chen, Y., Dilley, J., Li, Y., Embry, M., Zhang, H., Nguyen, N., Amin, P., Oh, J., and Henderson, D.R. (2001). Antitumor synergy of CV787, a prostate cancer-specific adenovirus, and paclitaxel and docetaxel. *Cancer Res.* 61, 517–525.